FARADAY

Temperature dependence of the rate constant and branching ratio for the OH + ClO reaction

Jennifer B. Lipson, Matthew J. Elrod, Thomas W. Beiderhase, Luisa T. Molina and Mario J. Molina

Departments of Earth, Atmospheric and Planetary Sciences and of Chemistry, Massachusetts Institute of Technology, Cambridge, MA 02139, USA

The overall rate constant and branching ratio for the OH + ClO reaction have been measured using the turbulent flow technique with high-pressure chemical ionization mass spectrometry for the detection of reactants and products. At 298 K and *ca.* 100 Torr pressure, the overall rate constant was determined to be $(1.46 \pm 0.23) \times 10^{-11}$ cm^3 molecule^{-1} s^{-1}. The temperature dependence of the rate constant was investigated between 205 and 298 K, yielding the following Arrhenius expression: $(5.5 \pm 1.6) \times 10^{-12}$ exp[$(292 \pm 72)/T$] cm^3 molecule^{-1} s^{-1}. For the branching ratio studies OD was used instead of OH, making it possible to observe directly the production of DCl from the minor channel of the OD + ClO reaction. The temperature dependence of the rate constant for this minor channel was investigated between 210 and 298 K, yielding the following Arrhenius expression: $(1.7 \pm 0.3) \times 10^{-13}$ exp[$(363 \pm 50)/T$] cm^3 molecule^{-1} s^{-1}. The branching ratio for the DCl channel was found to range from 0.05 ± 0.02 at 298 K to 0.06 ± 0.02 at 210 K.

The reaction of OH with ClO potentially plays an important role in the partitioning of chlorine in the stratosphere. Although the major products of the OH + ClO reaction are HO_2 and Cl ($\Delta H^\circ_{298\,K} = -1.7$ kcal mol^{-1}),

$$OH + ClO \rightarrow HO_2 + Cl \quad (1a)$$

the reaction may have a minor channel that produces HCl and O_2 ($\Delta H^\circ_{298\,K} = -55.8$ kcal mol^{-1}):

$$OH + ClO \rightarrow HCl + O_2 \quad (1b)$$

Reaction (1b) is thermodynamically feasible, but kinetically disfavoured because two bonds need to be broken almost simultaneously; it most likely proceeds through a four-centred transition state. The conversion of ClO to Cl in reaction (1a) is a chain-propagating step in catalytic ozone depletion cycles because ClO and Cl are both active forms of chlorine. For example, Cl and ClO participate in the ozone depletion cycle:

$$Cl + O_3 \rightarrow ClO + O_2$$

$$ClO + O \rightarrow Cl + O_2$$

$$\text{net:} \quad O + O_3 \rightarrow 2O_2$$

However, reaction (1b) converts an active form of chlorine (ClO) into a more stable reservoir species (HCl). Since reaction (1b) is a chain-terminating step, even a relatively small branching ratio may lead to substantially less ozone depletion by chlorine-containing compounds.

Recent attempts to model ozone levels in the upper stratosphere have resulted in an overprediction of ozone loss rates by as much as 35% at 40 km.[1–6] The inability to correctly simulate the amount of O_3 is largely due to the fact that modelling studies have been unable to reproduce measured stratospheric mixing ratios of ClO and HCl.[2–8] The models tend to overestimate the ClO/HCl ratio between 20 and 50 km by as much as 40%,[7] possibly indicating that the models are missing a source of HCl production in the stratosphere. Since calculated O_3 levels are very sensitive to the partitioning of chlorine, an overprediction of active chlorine (ClO) will lead to an underestimation of O_3. Several studies have proposed that the discrepancy between field measurements and modelling studies could be resolved by including the minor channel of the OH + ClO reaction (1b) as a source of HCl production in the models.[2,3,5,6,8] In the most recent study, Michelsen *et al.*[8] found that including a 7% branching ratio [$k_{1b}/(k_{1a} + k_{1b})$] in their model resulted in agreement between measured and modelled profiles of [HCl], [$ClNO_3$] and [ClO] at nearly all altitudes and latitudes. Furthermore, Michelsen *et al.* concluded that uncertainties in the rate constants of other important reactions involving HCl, such as $Cl + CH_4 \rightarrow HCl + CH_3$ and $OH + HCl \rightarrow Cl + H_2O$, cannot fully account for the observed errors in calculated chlorine partitioning.

Previous attempts to measure the branching ratio of the OH + ClO reaction have been unable to rule out an HCl yield of zero for the minor channel due to uncertainties in the results.[9–12] The laboratory studies were not able to directly observe a product from reaction (1b) due to either the inability to detect HCl and O_2 [9–11] or due to insufficient sensitivity for HCl.[12] Because of the indirect methods used in some studies[9,10] and the large uncertainties in all of the measurements of the branching ratio, no consensus has been reached on the existence of channel (1b).

Some discrepancies also exist in the previous studies of the temperature dependence of the overall rate constant for the OH + ClO reaction.[9–13] Hills and Howard[11] report a slight negative temperature dependence, but two other studies[10,13] found that the rate constant was independent of temperature. All previous studies of the rate constant and the branching ratio were conducted at low pressure (*ca.* 1 Torr) due to the limitations inherent in the conventional discharge laminar flow tube technique. As pointed out by Wennberg *et al.*,[14] the interpretation of field measurements of important atmospheric species is hindered by uncertainties in the laboratory-measured rate constants due to the fact that most of the studies have not been carried out under pressure and temperature conditions characteristic of the stratosphere. In this article we describe our investigation of the kinetics and branching ratio of reaction (1) conducted at pressures near 100 Torr and at a range of temperatures extending to those found in the lower stratosphere using a turbulent flow tube coupled to a high-pressure chemical ionization mass spectrometer. We have previously shown that the turbulent flow tube technique, developed in our laboratory, can be used to accurately determine the rate constants of reactions at pressures ranging from 50 to 760 Torr and at temperatures as low as

180 K.[15–17] As in our recent studies of $HO_2 + NO$[18] and $HO_2 + BrO$,[19] we employed high-pressure chemical ionization mass spectrometry to monitor with high sensitivity various species relevant to the OH + ClO reaction.

Experimental

A schematic diagram of the experimental apparatus is presented in Fig. 1 and is similar to that used in our previous studies.[18,19] The flow tube (2.2 cm i.d., 120 cm long) was constructed of Pyrex tubing and coated with Halocarbon wax. A large flow of nitrogen carrier gas (*ca.* 50 STP l min^{-1}) was injected at the rear of the flow tube. For the kinetics experiments, the gases necessary to generate ClO were introduced through a sidearm (10 cm long, 12.5 mm diameter) located at the rear of the flow tube. OH(D) was generated in a triple nested movable injector which consisted of an inner 3 mm Pyrex tube, a middle 6 mm Pyrex tube and an outer encasement made from corrugated Teflon tubing. The outer encasement was used so that the injector could be moved to various injector positions without breaking any vacuum seals, as well as to prevent ambient gases from condensing on cold portions of the injector. A fan-shaped Teflon device was placed at the end of the injector in order to enhance turbulent mixing. For the branching ratio experiments the OH(D) was generated in the side arm and the ClO was generated in the injector. The electric discharge ion source was placed between the temperature regulated flow tube and the inlet to the quadrupole mass spectrometer. A 1.7 mm aperture between the flow tube and the ion–molecule region created a pressure drop from 100 Torr in the flow tube to 15 Torr in the ion–molecule region. The pressures in the two regions were measured using MKS capacitance manometers (1000 Torr full scale). All gas flows were monitored with calibrated Tylan General mass flow meters. For the low temperature studies, HCFC-123 was used in a coolant for the jacketed flow tube, and the nitrogen carrier gas was also precooled by passing it through a copper coil immersed in either an ice–water or a liquid-N_2 reservoir followed by resistive heating. The temperature was controlled as the reaction region to within 1 K; it was determined at both the entrance and exit points of the temperature regulated region of the flow tube using copper–constantan thermocouples.

The following gases were used as supplied or after further purification as described below: helium (99.999%), O_2 (99.994%), H_2 (99.999%), D_2 (99.995%), Cl_2 (>99.9%), NO_2 (99.5%), NO (CP grade) and C_2H_6 (CP Grade).

Bimolecular rate constants were measured using the pseudo-first-order approximation method with ClO as the excess reagent. ClO was generated using the following reaction ($k_2 = 1.2 \times 10^{-11}$ cm^3 $molecule^{-1}$ s^{-1}):[20]

$$Cl + O_3 \rightarrow ClO + O_2 \quad (2)$$

Chlorine atoms were produced by combining a 2.0 STP l min^{-1} flow of helium, which had passed through a molecular sieve trap immersed in liquid nitrogen, with a 0.3–3.0 STP ml min^{-1} flow of a 5% Cl_2–He mixture which then passed through a microwave discharge produced by a Beenakker cavity operating at 70 W. To generate ClO, the chlorine atoms were then injected into a 20 cm long piece of 6 mm Teflon tubing connected to the side arm and mixed with an excess of O_3 (*ca.* 10^{13} molecule cm^{-3}) in order to ensure that only negligible amounts of chlorine atoms were introduced into the main flow. The large excess of O_3 also helped to scavenge Cl atoms produced by the main channel of the title reaction, and therefore helped to minimize the reverse reaction:

$$Cl + H(D)O_2 \rightarrow OH(D) + ClO \quad (3)$$

which could have affected the pseudo-first-order decays of OH(D) ($k_3 = 9.1 \times 10^{-12}$ cm^3 $molecule^{-1}$ s^{-1}).[20] The O_3 was generated by passing O_2 through an OREC ozonator and then the O_3 was stored in a silica gel trap immersed in a dry ice–ethanol bath. O_3 was introduced into the system by passing a 5.0–20.0 STP ml min^{-1} flow of N_2 through the trap. Ozone partial pressures were determined by UV absorbance at 253.7 nm (Penray Hg lamp) in a 0.98 cm flow-through quartz cell. Absolute ClO concentrations were determined by the titration reaction ($k_4 = 1.7 \times 10^{-11}$ cm^3 $molecule^{-1}$ s^{-1}):[20]

$$ClO + NO \rightarrow NO_2 + Cl \quad (4)$$

and subsequent calibration of the NO_2 mass spectrometer signal. The NO was purified, using a method similar to that described in our previous study,[18] in order to reduce the background NO_2 contribution. To accurately determine ClO concentrations *via* reaction (4), it was necessary to scavenge the Cl atoms produced by the titration reaction in order to prevent regeneration of ClO due to the excess of O_3 used in the experiments. An excess of ethane (*ca.* 3×10^{13} molecule cm^{-3}) injected at the rear of the flow tube was used to scavenge the Cl atoms:

$$C_2H_6 + Cl \rightarrow C_2H_5 + HCl \quad (5)$$

Ethane was chosen as a scavenger because of its relatively fast rate of reaction with Cl ($k_5 = 5.7 \times 10^{-11}$ cm^3 $molecule^{-1}$ s^{-1}, almost 5 times faster than the $O_3 + Cl$ reaction).[20] The HCl product of reaction (5) is stable and does not interfere with the titration chemistry. However, the C_2H_5 product

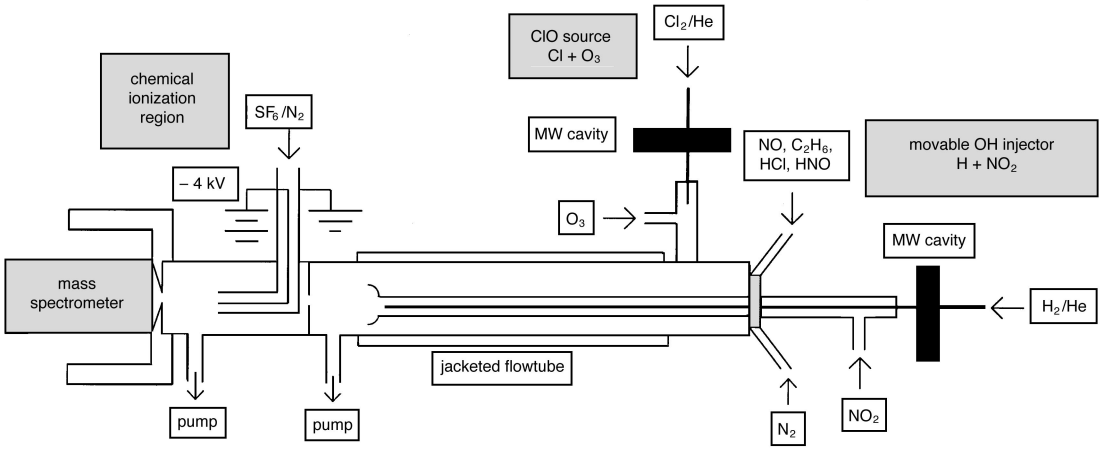

Fig. 1 Schematic diagram of experimental apparatus

reacts with NO_2 ($k_6 = 4.5 \times 10^{-11}$ cm^3 molecule^{-1} s^{-1}):[21]

$$C_2H_5 + NO_2 \rightarrow \text{products} \quad (6)$$

which results in a slight underestimation of the ClO concentration. Modelling of the titration reaction system was used to correct for this underestimation and in almost all cases the correction factor was <15%. A sample ClO calibration curve is shown in Fig. 2. For this study, ClO concentrations ranged from 0.5 to 3.0x10^{12} molecule cm^{-3}.

OH(D) was generated by the following reaction ($k_7 = 1.3 \times 10^{-10}$ cm^3 molecule^{-1} s^{-1}):[20]

$$H(D) + NO_2 \rightarrow OH(D) + NO \quad (7)$$

Because OH(D) was introduced through a movable injector where the corresponding concentrations are *ca.* 40 times higher than in the main flow tube, its reaction with NO_2 ($k_8 = 4.2 \times 10^{-12}$ cm^3 molecule^{-1} s^{-1} at 100 Torr):[20]

$$OH(D) + NO_2 + M \rightarrow H(D)NO_3 + M \quad (8)$$

is a concern in the production of OH(D) by reaction (7). By taking advantage of the long lifetime of H(D) atoms, this difficulty was surmounted by using a nested injector, which kept the H(D) atoms (entrained in the inner 3 mm Pyrex tube) and NO_2 molecules (entrained in the outer 6 mm Pyrex tube) separate throughout all but the last 1 cm of the injector. The H(D) atoms were allowed to mix with an excess of NO_2 (4.0×10^{13} molecule cm^{-3} inside the injector) for only about 1 ms, allowing reaction (7) to virtually go to completion, but preventing significant loss of OH(D) due to reaction (8). H(D) atoms were generated by combining a 1.0 STP l min^{-1} flow of helium with a 0.1–0.4 STP ml min^{-1} flow of a 2% H_2 or D_2–He mixture, which then passed through a molecular sieve trap immersed in liquid nitrogen and finally through a microwave discharge produced by a Beenakker cavity operating at 70 W. Although reaction (8) was minimized in the production of OH(D), this reaction proved to be a convenient titration method for determining absolute concentrations of OH(D). An excess of NO_2 was used to convert all of the OH(D) into $H(D)NO_3$ followed by calibration of the $H(D)NO_3$ mass spectrometer signal using a bubbler containing 60% HNO_3 solution by weight, immersed in an ice–water bath. The vapour pressure of HNO_3 for this solution at 0 °C is 0.2 Torr.[22] In determining the absolute concentrations of OD, it was assumed that the DNO_3 and HNO_3 mass spectrometer signals had the same sensitivity. The HNO_3 solution from the bubbler was periodically titrated with NaOH to confirm the long-term stability of the solution. Even after several months of use the bubbler solution was found to have the same composition as the original stock solution. A sample OH calibration curve is shown in Fig. 3. OH(D) concentrations used in this study ranged from 0.5 to 2.0×10^{11} molecule cm^{-3}. In order to insure pseudo-first-order kinetic conditions, [OH(D)] was kept at most one-tenth as large as [ClO].

Owing to the large background of HCl produced by the ClO source, OD was used instead of OH in the majority of the branching ratio experiments. In these studies, production of DCl from reaction (1b) was observed directly over a reaction time of *ca.* 20 ms. Computer modelling was used to extract a rate constant for reaction (1b), using the initial measured concentrations of ClO, OD and all precursors, and then fitting the observed DCl production. For the branching ratio studies, ClO was generated by reaction (2) in a double nested movable injector. For these experiments, the chlorine atoms were produced by combining a 4.0 STP 1 min^{-1} flow of helium, which had passed through a molecular sieve trap immersed in liquid nitrogen, with a 0.3–1.0 STP ml min^{-1} flow of a 5% Cl_2–He mixture which then passed through a microwave discharge as described above. To generate ClO, the chlorine atoms were mixed with an excess of O_3 (*ca.* 10^{13} molecule cm^{-3}) throughout the whole length of the movable injector to ensure minimal concentrations of chlorine atoms in the main flow. The large excess of O_3 also helped to scavenge Cl atoms produced by the main channel of reaction (1), and therefore helped to minimize production of background DCl due to the reaction:

$$DO_2 + Cl \rightarrow DCl + O_2 \quad (9)$$

Since reaction (9) is relatively fast ($k_9 = 3.2 \times 10^{-11}$ cm^3 molecule^{-1} s^{-1}),[20] and DO_2 and Cl are the major products of the OD + ClO reaction, reaction (9) was found to be the largest potential source of DCl background. Absolute ClO concentrations were measured using the technique described earlier.

For the branching ratio studies, OD was generated by reaction (7) in the side arm of the flow tube. D atoms were generated by combining a 0.2 STP 1 min^{-1} flow of helium with a 0.1–0.4 STP ml min^{-1} flow of a 2% D_2–He mixture through a microwave discharge as described above. The D atoms were then mixed with an excess of NO_2 (1.0×10^{12} molecule cm^{-3}) to ensure that practically no D atoms were introduced into the main flow. The experimental conditions were optimized in

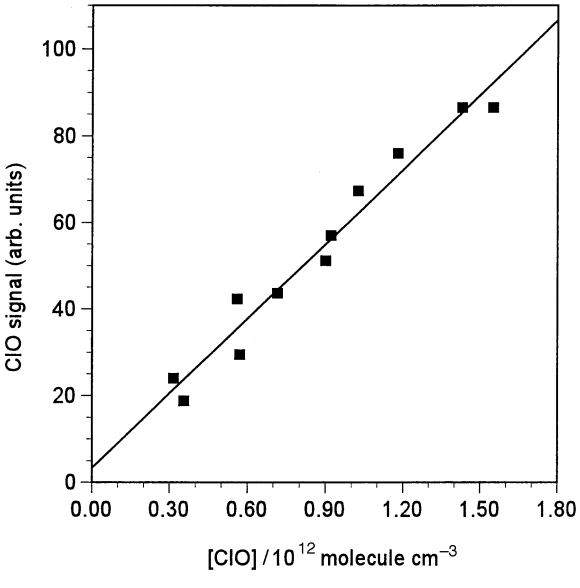

Fig. 2 ClO calibration plot

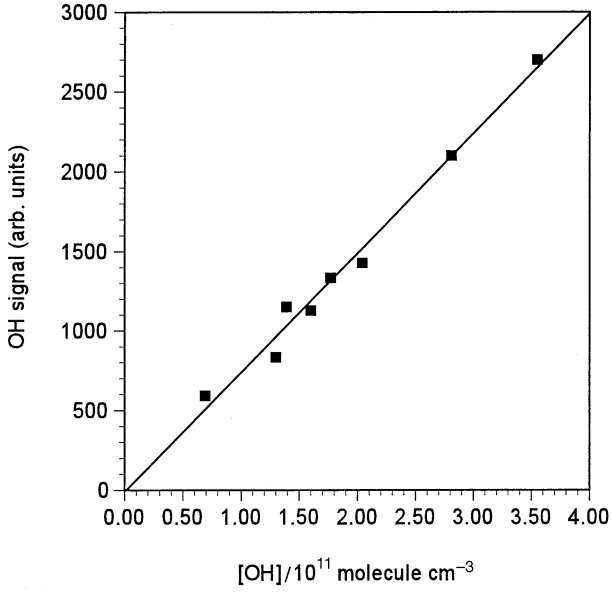

Fig. 3 OH calibration plot

order to minimize background DCl production from the reaction of D with Cl_2 ($k_{10} = 1.4 \times 10^{-11}$ cm^3 molecule^{-1} s^{-1}):[21]

$$D + Cl_2 \rightarrow DCl + Cl \quad (10)$$

Absolute DCl concentrations were determined by calibration of the DCl mass spectrometer signal using a bubbler containing 20% DCl–D_2O solution by weight, immersed in an ice–water bath. The vapour pressure of HCl for a 20% HCl–H_2O solution by weight at 0 °C is 0.038 Torr.[23] For the DCl calibration it was assumed that the 20% DCl solution had the same vapour pressure as the 20% HCl solution. An intercomparison of two bubblers, one containing a 20% DCl solution and the other containing a 20% HCl solution, showed that the DCl and HCl mass spectrometer signals were in very good agreement for the same nitrogen flow. At low temperatures the DCl from the bubbler took a long time to equilibrate. For reasons of convenience, calibrations of the DCl signal at low temperatures were also made by reacting an excess of D atoms with a known amount of Cl_2. The two methods of DCl calibration were in very good agreement.

Most of the chemical species relevant to this study were chemically ionized with the SF_6^- reagent ion and then detected with the quadrupole mass spectrometer as described in our earlier publications.[18,19] SF_6^- was produced in the ion source by combining a 2.5 STP l min^{-1} flow of nitrogen with a 0.4 STP ml min^{-1} flow of a 5% SF_6–N_2 mixture which then passed over the electric discharge. In the chemical ionization scheme employed here, OH(D), ClO, Cl, Cl_2, O_3 and NO_2 are detected as their parent negative ions by charge-transfer reactions with SF_6^-:

$$SF_6^- + OH(D) \rightarrow SF_6 + OH(D)^- \quad (11)$$

$$SF_6^- + ClO \rightarrow SF_6 + ClO^- \quad (12)$$

$$SF_6^- + Cl \rightarrow SF_6 + Cl^- \quad (13)$$

$$SF_6^- + Cl_2 \rightarrow SF_6 + Cl_2^- \quad (14)$$

$$SF_6^- + O_3 \rightarrow SF_6 + O_3^- \quad (15)$$

$$SF_6^- + NO_2 \rightarrow SF_6 + NO_2^- \quad (16)$$

The rate constant for reaction (11) has been estimated by Lovejoy *et al.*[24] to be 2×10^{-9} cm^3 molecule^{-1} s^{-1}. The rate constants for reactions (12) and (13) have not been measured. The rate constants for reactions (14), (15) and (16) are 1.1×10^{-10}, 1.2×10^{-9} and 1.4×10^{-10} cm^3 molecule^{-1} s^{-1}, respectively.[25] H(D)Cl and H(D)NO_3 are detected as H(D)ClF^- and H(D)NO_3F^- through fluoride-transfer reactions with SF_6^-:

$$SF_6^- + H(D)Cl \rightarrow SF_5 + H(D)ClF^- \quad (17)$$

$$SF_6^- + H(D)NO_3 \rightarrow SF_5 + H(D)NO_3F^- \quad (18)$$

The rate constants for reactions (17) and (18) are 1.5×10^{-9} and 2.0×10^{-9} cm^3 molecule^{-1} s^{-1}, respectively.[25] H(D)O_2 is detected as $SF_4O_2^-$, generated presumably through a multistep pathway. The ion–molecule region was kept at a lower pressure (15 Torr) than the neutral flow tube (100 Torr). The drop in pressure lowered the concentrations of the neutrals in the ion–molecule region, thus decreasing the rates of potential ion–molecule side-reactions. In our previous study of HO_2 + NO,[18] we reported that the OH^- mass spectrometer signal was not proportional to [OH] possibly due to secondary reactions. It is likely that those secondary reactions were taking place in the ion–molecule region, which was kept at the same pressure as the neutral flow tube (70–190 Torr). In this study, we found that the $OH(D)^-$ signal was proportional to [OH(D)] as determined by titration with NO_2 and subsequent calibration of the H(D)NO_3 mass spectrometer signal. Presumably, the lower concentrations of neutrals in the ion–molecule region helped to decrease secondary reactions involving OH^-, therefore making it possible to use this signal for detection of OH. The lower neutral concentrations in the ion–molecule region also helped to prevent depletion of the SF_6^- reagent ions due to reaction with species in large excess, such as O_3.

Results and Discussion

In our earlier work, we reported that our chemical ionization detection scheme resulted in sensitivities of 100, 200 and 1000 ppt (at 100 Torr) for NO_2, HO_2 and OH, respectively.[18] Although we did not carry out formal calibrations of the mass spectrometer for all the chlorine species detected with this method (Cl_2, ClO, Cl), it was apparent that these species could be detected with a similar sensitivity to that obtained for NO_2. The mass spectrometer signals for these compounds were found to be linear over the range of concentrations used in this work. The stated sensitivity was more than adequate for the present work; actually, it was necessary to degrade the sensitivity of the spectrometer (by decreasing the ion–molecule reaction time) to allow the introduction of greater amounts of reactants, which were necessary to study the relatively slow OH + ClO reaction, without depleting the SF_6^- reagent ions or inducing complications from secondary ion–molecule processes.

Overall rate constant

Bimolecular rate constants were obtained *via* the usual pseudo-first-order approximation method, using ClO as the excess reagent. Typical OH decay curves as a function of injector distance are shown in Fig. 4. The first-order rate constants obtained from fitting the OH decay curves were plotted against [ClO] in order to determine the bimolecular rate constant, as shown in Fig. 5. This approach for determining bimolecular rate constants assumes that deviations from the plug flow approximation are negligible. Under the conditions present in our turbulent flow tube, Seeley *et al.*[18] estimated that these deviations result in apparent rate constants which are at most 8% below the actual values. Hence, the flow corrections were neglected as they are smaller than the sum of the other likely systematic errors in the measurements of gas flows, temperature, detector signal, pressure and absolute ClO concentrations. Indeed, we consider the major source of error

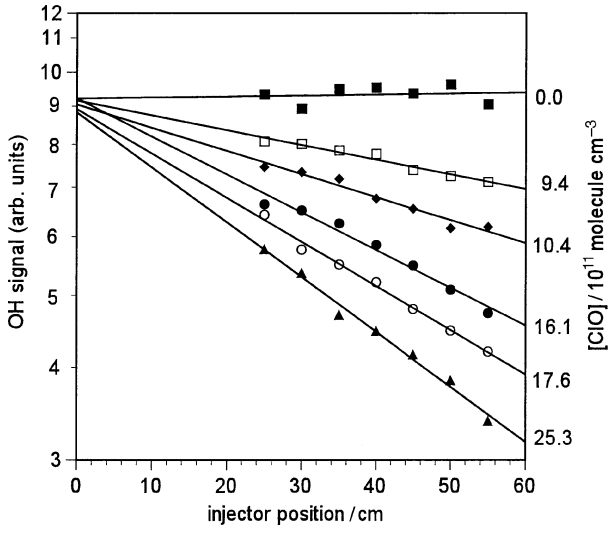

Fig. 4 Typical set of OH signals as a function of injector distance. This data set was obtained under the following conditions: $P = 100$ Torr; $T = 298$ K, average velocity = 2100 cm s^{-1}; Reynolds number = 4010.

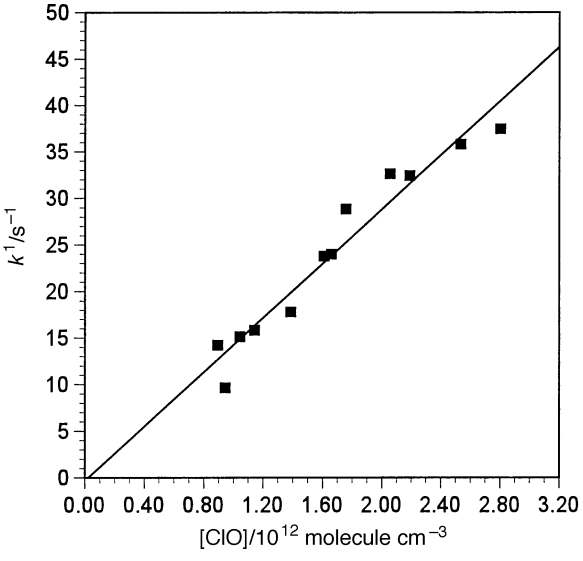

Fig. 5 Typical plot of k^1 as a function of [ClO]. This plot was obtained under the same conditions as listed in Fig. 4.

in our experiments to arise from the determination of [ClO] from the titration procedure outlined above. Considering such sources of error, we estimate that rate constants can be determined with an accuracy of $\pm 30\%$ (2σ).

A complete list of experimental conditions and measured rate constants is presented in Table 1. We performed four separate determinations of the overall rate constant for OH + ClO at 298 K and arrived at the mean value of $k_1 = (1.46 \pm 0.23) \times 10^{-11}$ cm^3 molecule^{-1} s^{-1}; the uncertainty represents the two standard deviation statistical error in the data and is not an estimate of systematic errors. Table 2 contains a comparison of all reported rate constants for the OH + ClO reaction. Our value lies roughly in the middle of the range of reported rate constants at 298 K, and the overlap of uncertainty ranges makes our work consistent with all previous measurements except the lowest value reported by Leu and Lin.[9] However, as Hills and Howard[11] have pointed out, the reported values of Leu and Lin are probably too low because these authors did not correct their results for the effect of OH regeneration by reaction (3). A correction is necessary because Leu and Lin used an excess of Cl in their production of ClO by reaction (2) or by the reaction Cl + $Cl_2O \rightarrow ClO + Cl_2$. Ravishankara *et al.*[13] also used an excess of Cl in the production of ClO, and they reported a 26% correction factor due to OH regeneration. The regeneration of OH was not a concern in our experiments because the excess of O_3 used to produce ClO in our system effectively scavenged Cl atoms, including those produced by reaction (1a). A second reason why the value of Leu and Lin may be too low is that they did not perform absolute titrations of ClO. Leu and Lin and also Ravishankara *et al.* assumed that the concentrations of ClO produced were equal to the initial concentrations of O_3 or Cl_2O as determined by optical absorption. However, neither study took into account possible loss mechanisms for ClO, such as self-reaction or wall loss. The loss of ClO in a small diameter inlet has been observed to be as large as 50%.[12] An overestimation of ClO concentrations will lead to an underestimation of the rate constant. In our experiments the ClO concentrations were determined by absolute titration, as described in the Experimental section. The good agreement between our reported rate constant at 100 Torr and previous measurements made at low pressure (*ca.* 1 Torr) suggests that the overall rate of reaction (1) does not have a significant pressure dependence.

Table 1 Summary of experimental conditions and measured overall rate constants for OH + ClO

T/K	P/Torr	velocity /cm s^{-1}	Reynolds number	$k \pm 2\sigma$ /10^{-11} cm^3 molecule^{-1} s^{-1}
298	97	2120	3910	1.36 ± 0.32
298	100	2100	4010	1.46 ± 0.22
298	91	2060	3510	1.47 ± 0.24
298	93	1950	3510	1.53 ± 0.12
280	92	2140	4100	1.72 ± 0.34
252	93	2080	4880	1.58 ± 0.46
247	90	1980	4600	1.80 ± 1.06
243	95	1960	5100	1.66 ± 0.80
234	96	2090	5750	1.90 ± 0.32
224	94	1920	5600	1.91 ± 0.56
224	93	2070	5980	2.15 ± 0.32
215	94	2025	6450	2.26 ± 0.38
214	92	1980	6200	1.97 ± 0.54
208	93	2050	7020	2.38 ± 0.62

We performed several measurements of the overall rate constant for OH + ClO at temperatures between 205 and 298 K in order to establish the temperature dependence of the rate constant for conditions relevant to the stratosphere. From the data listed in Table 1 and plotted in Fig. 6, we obtain the Arrhenius expression $k(T) = (5.5 \pm 1.6) \times 10^{-12}$ exp[$(292 \pm 72)/T$] cm^3 molecule^{-1} s^{-1}. Compared to the results of Hills and Howard,[11] our calculated negative activation energy is *ca.* 25% larger and our preexponential factor is *ca.* 30% smaller. However, these differences result in only a *ca.* 10% difference in the rate constant at stratospheric temperatures, compared to the value of Hills and Howard; given the range of uncertainties, the agreement is very good. The two other temperature dependence studies of the OH + ClO reaction reported that the overall rate was independent of temperature.[10,13] Ravishankara *et al.* did measure a small negative temperature dependence, but they chose to report that k_1 was temperature independent because their temperature coefficient was not statistically significant due to the large uncertainty.

We also measured the overall rate constant for the OD + ClO reaction at temperatures between 200 and 298 K, using the same method as described above for the OH + ClO reaction. Table 3 presents a complete list of experimental conditions and measured rate constants for the OD + ClO reaction. From the data listed in Table 3, we obtain the Arrhenius

Table 2 Comparison of measured overall rate constants for OH + ClO

technique[a]	T/K	P/Torr	$k_{298\,K}$/10^{-11} cm^3 molecule^{-1} s^{-1}	E_a/R/K	ref.
DF-LF/RF	298	1.0–3.5	0.91 ± 0.13	—	9
DF-LF/RF	248–335	1.0	1.17 ± 0.33	−66	13
DF-LF/RF	243–298	1.0–5.0	1.19 ± 0.32	—	10
DF-LF/LMR	219–373	1.0	1.75 ± 0.31	−235	11
DF-LF/LIF	298	0.5–0.9	1.94 ± 0.38	—	12
DF-TF/CIMS	205–298	100	1.46 ± 0.23	−292	this work

[a] DF, discharge flow; LF, laminar flow; TF, turbulent flow; RF, resonance fluorescence detection; LMR, laser magnetic resonance detection; LIF, laser-induced fluorescence detection; CIMS, chemical ionization mass spectrometry detection.

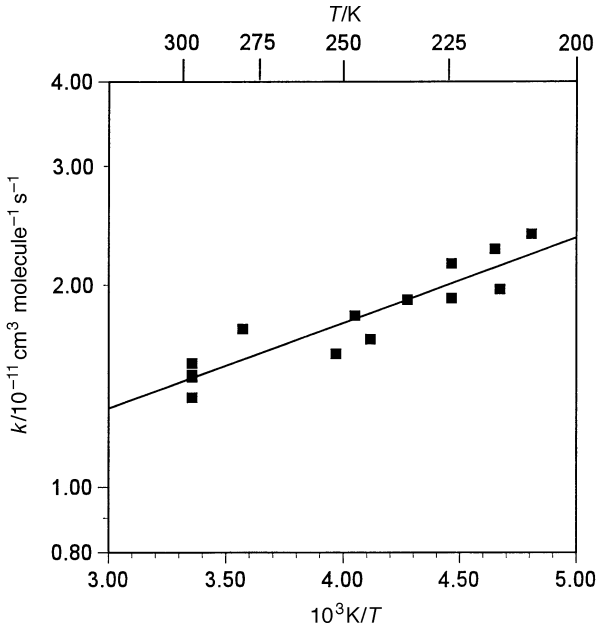

Fig. 6 Arrhenius plot for the overall reaction OH + ClO; the least-squares fit to the data yields the expression $k(T) = (5.5 \pm 1.6) \times 10^{-12}$ exp[(292 ± 72)/T] cm^3 molecule^{-1} s^{-1}

expression $k(T) = (4.2 \pm 2.0) \times 10^{-12}$ exp[(280 ± 114)/T] cm^3 molecule^{-1} s^{-1}. There have been no previous studies of this reaction. The Arrhenius expressions for OH + ClO and OD + ClO are similar, indicating that the isotope effect on the overall rate of reaction (1) is small.

Branching ratio

The large background level of HCl (*ca.* 10^{11} molecule cm^{-3}) from the ClO source made it difficult to detect small amounts of HCl produced by reaction (1b) over the reaction time. The HCl background in our system is due most likely to trace impurities of H_2 in the helium sweep gas used to flush Cl_2 through the microwave discharge in the ClO source. Although 99.999% pure helium was used, the manufacturer specifications indicate levels of H_2 up to 1 ppm. If 1 ppm of H_2 (*ca.* 10^{12} molecule cm^{-3}) is present and sent through the microwave discharge in the presence of chlorine, it could certainly produce enough H atoms to create background HCl levels of the order of 10^{11} molecule cm^{-3}. This problem can be solved, for example, by using a thermal dissociation source for chlorine instead of a microwave discharge source. We are currently conducting additional experiments using this alternative Cl-atom source, which was employed in our laboratory previously.[26]

Table 3 Summary of experimental conditions and measured overall rate constants for OD + ClO

T/K	P/Torr	velocity /cm s^{-1}	Reynolds number	$k \pm 2\sigma$ /10^{-11} cm^3 molecule^{-1} s^{-1}
298	99	1840	3460	0.91 ± 0.22
298	90	1920	3200	1.09 ± 0.26
298	91	2000	3540	1.17 ± 0.20
262	98	2090	4770	1.45 ± 0.28
252	94	2090	4910	1.21 ± 0.34
242	90	1800	4250	1.29 ± 0.24
233	90	2045	5290	1.48 ± 0.44
224	91	2080	5870	1.31 ± 0.20
223	92	2050	5700	1.54 ± 0.16
212	91	1840	5800	1.47 ± 0.28
204	90	2060	6820	1.75 ± 0.14

Because of the uncertainty created by a large HCl background, we used OD instead of OH in the majority of the branching ratio experiments. Since there is almost no DCl background from the ClO source, we were able to observe production of very small concentrations of DCl (*ca.* 10^9 molecule cm^{-3}) over the reaction time (*ca.* 20 ms) which we have positively identified as coming from reaction (1b). Fig. 7 shows that the rise of DCl is easily observed above the small background noise. Under the optimal experimental conditions ([ClO] ≈ 1×10^{12} molecule cm^{-3} and [OD] ≈ 1×10^{11} molecule cm^{-3}), modelling shows that side reactions can only produce concentrations of DCl (*ca.* 10^8 molecule cm^{-3}) that are less than the detection limit of the instrument (*ca.* 50 ppt). Table 4 contains a list of the reactions used in the modelling. The following side-reactions can produce DCl in our system:

$$DO_2 + Cl \rightarrow DCl + O_2 \quad (9)$$

$$D + Cl_2 \rightarrow DCl + Cl \quad (10)$$

$$Cl + D_2 \rightarrow DCl + D \quad (19)$$

In our experiments, the source conditions for OD and ClO are optimized in order to prevent stray D and Cl atoms from entering the main flow tube. Modelling of the OD source shows that the concentration of D atoms is so small that reaction (10) is negligible as a source of DCl. Furthermore, reaction (19) is too slow to be important in our reaction system ($k_{19} = 1.6 \times 10^{-14}$ cm^3 molecule^{-1} s^{-1}).[21] Reactions (10) and (19) combine to produce DCl concentrations far below the detection limit of the instrument ([DCl] ≈ 10^6 molecule cm^{-3}). Reaction (9) is more difficult to avoid because DO_2 and Cl are the products of reaction (1a), the main channel of the OD + ClO reaction. However, modelling shows that the large excess of O_3, used to generate ClO, is efficient in scavenging Cl atoms produced in the main flow tube. Under optimal experimental conditions, reaction (9) produces levels of DCl (*ca.* 10^8 molecule cm^{-3}) that are below the detection limit of the instrument.

As stated in the Experimental section, computer modelling was used to extract a rate constant for reaction (1b) by fitting the observed DCl production. The model input included the

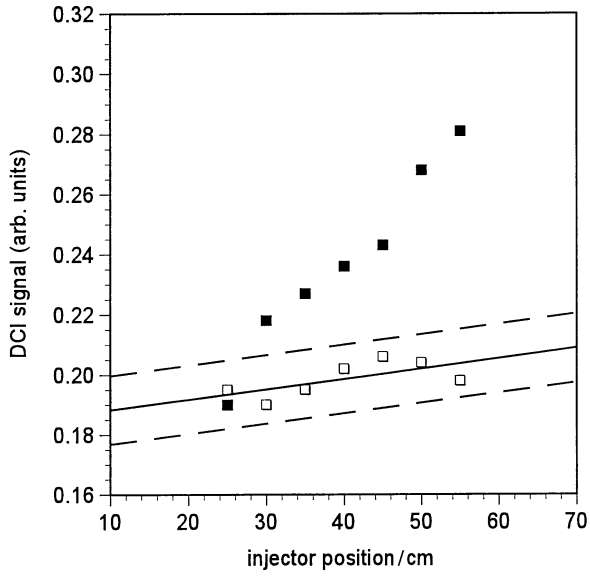

Fig. 7 Observed production of DCl ([DCl] = 1.4×10^9 molecule cm^{-3}) from reaction (1b) (■) above the small DCl background level (□) as a function of injector distance. A least-squares fit to the DCl background data was performed, and the dotted lines represent the $\pm 2\sigma$ level. This data set was obtained under the following conditions: P = 96 Torr; T = 298 K; average velocity = 1975 cm s^{-1}; Reynolds number = 3350; $[OD]_0 = 1.42 \times 10^{11}$ molecule cm^{-3}; $[ClO]_0 = 8.3 \times 10^{11}$ molecule cm^{-3}.

Table 4 Chemical reactions used in computer simulations for the branching ratio studies

reaction	k^a /cm^3 molecule^{-1} s^{-1}
$OD + ClO \rightarrow DO_2 + Cl$	1.1×10^{-11}
$OD + ClO \rightarrow DCl + O_2$	see text
$Cl + DO_2 \rightarrow DCl + O_2$	3.2×10^{-11}
$Cl + DO_2 \rightarrow OD + ClO$	9.1×10^{-12}
$Cl + O_3 \rightarrow ClO + O_2$	1.2×10^{-11}
$Cl + D_2 \rightarrow DCl + D$	1.6×10^{-14}
$Cl + NO_2 + M \rightarrow ClONO + M$	3.4×10^{-12}
$D + Cl_2 \rightarrow DCl + Cl$	1.3×10^{-11}
$D + O_3 \rightarrow OD + O_2$	2.9×10^{-11}
$D + NO_2 \rightarrow OD + NO$	1.3×10^{-10}
$OD + O_3 \rightarrow DO_2 + O_2$	6.8×10^{-14}
$OD + Cl_2 \rightarrow DOCl + Cl$	6.7×10^{-14}
$OD + OD \rightarrow D_2O + O$	1.5×10^{-12}
$OD + OD + M \rightarrow D_2O_2 + M$	1.4×10^{-12}
$OD + DO_2 \rightarrow D_2O + O_2$	1.1×10^{-10}
$OD + NO_2 + M \rightarrow DNO_3 + M$	4.2×10^{-12}
$OD + NO + M \rightarrow DONO + M$	1.4×10^{-12}
$OD + DCl \rightarrow D_2O + Cl$	1.3×10^{-13}
$ClO + ClO \rightarrow$ products	7.7×10^{-14}
$ClO + DO_2 \rightarrow DOCl + O_2$	5.0×10^{-12}
$ClO + NO \rightarrow NO_2 + Cl$	1.7×10^{-11}
$ClO + NO_2 + M \rightarrow ClONO_2 + M$	4.8×10^{-13}
$DO_2 + DO_2 \rightarrow D_2O_2 + O_2$	6.0×10^{-13}
$DO_2 + NO_2 + M \rightarrow DO_2NO_2 + M$	4.0×10^{-13}
$DO_2 + NO \rightarrow NO_2 + OD$	1.1×10^{-11}

[a] Rate constants are from ref. 20 and ref. 21, at 298 K and 100 Torr.

initial concentrations of ClO, OD and of all precursors. The branching ratio for the OD + ClO reaction was measured at room temperature under a variety of conditions to ensure that the results were independent of the initial concentrations. Table 5 contains a list of the initial conditions and calculated rate constants (k_{1b}) for these experiments. The fitting procedure used to calculate k_{1b} is obviously sensitive to the initial concentrations of OD and ClO and to the observed concentration of DCl produced over a specific reaction time. These concentrations were measured to better than 30% accuracy; we found that these errors propagate linearly into the calculated branching ratio. In experiment 1, the optimal initial concentrations for OD and ClO were used, such that the observed DCl production was due to reaction (1b) only. In experiment 2, the initial OD concentration was more than tripled compared to experiment 1. Under these conditions, modelling shows that *ca.* 20% of the observed DCl production was due to the side-reaction $DO_2 + Cl$. Despite the very different initial conditions and the differing amounts of DCl production from side-reactions, experiments 1 and 2 yielded very similar rate constants (5.3×10^{-13} and 5.6×10^{-13} cm^3 molecule^{-1} s^{-1}). Therefore, the modelling approach appears to correctly simulate the chemistry in our system, yielding branching ratio results which are independent of the initial conditions.

Although modelling shows that for optimal initial conditions the observed DCl production cannot be due to homogeneous side-reactions, the possibility exists that the DCl could be a result of heterogeneous reactions on the wall of the flow tube. Several experiments were performed that indicated that the observed DCl production was not due to heterogeneous processes. For most of the branching ratio studies a flow tube coated with Halocarbon wax was used in order to minimize OD wall loss. To check for a heterogeneous source of DCl, we performed one branching ratio experiment using an uncoated flow tube. If the DCl was being produced by heterogeneous reactions, an uncoated flow tube should lead to more observed DCl production, and therefore a larger calculated rate constant for reaction (1b). However, the results from experiment 5 for the uncoated flow tube show that the calculated rate constant [$k_{1b}(5) = 5.4 \times 10^{-13}$ cm^3 molecule^{-1} s^{-1}] is well within the range of rate constants obtained for the coated flow tube experiments. The excellent agreement between the coated and uncoated flow tube experiments indicates that the observed DCl production was not due to heterogeneous reactions on the wall of the flow tube.

A second experiment was performed to investigate the possibility of heterogeneous DCl production, in which we increased the total pressure in the flow tube by almost a factor of two. The molecular diffusion rate across the laminar sublayer at the walls of the flow tube decreases with increasing pressure;[15] therefore, the effects of heterogeneous processes are reduced at higher pressures. However, as shown in Table 5, the measured rate constant for reaction (1b) actually increased by *ca.* 35% at the higher pressure (180 *vs.* 95 Torr), at 298 and 227 K, indicating that the observed DCl production over the reaction time was not due to heterogeneous reactions. We are planning to conduct additional experiments to better establish the pressure dependency of the rate constant, which appears unusually large.

We performed several measurements of the branching ratio for OD + ClO at temperatures between 210 and 298 K in order to establish the temperature dependence of the rate constant k_{1b} for conditions relevant to the stratosphere. From the data listed in Table 5 (for 100 Torr pressure) and plotted in Fig. 8, we obtain the Arrhenius expression $k_{1b}(T) = (1.7 \pm 0.3) \times 10^{-13} \exp[(363 \pm 50)/T]$ cm^3 molecule^{-1} s^{-1}. The uncertainty represents the two standard deviation statistical error in the data and is not an estimate of systematic errors. The branching ratios (k_{1b}/k_1) reported in Table 5 were calculated using the measured Arrhenius expression for the overall rate of the OD + ClO reaction. At 100 Torr pressure, the

Table 5 Summary of experimental conditions and calculated rate constants (k_{1b}) for the branching ratio studies

expt. no.	T/K	P/Torr	$[OH]_0/10^{-11}$ molecule cm^{-3}	$[ClO]_0/10^{-12}$ molecule cm^{-3}	$k_{1b}/10^{-13}$ cm^3 molecule^{-1} s^{-1}	branching ratio (k_{1b}/k_1)
1	298	94	1.00	0.88	5.3	0.049
2	298	94	3.55	0.86	5.6	0.052
3	298	93	1.39	1.24	5.8	0.054
4	298	96	1.42	0.83	5.9	0.055
5[a]	298	93	1.85	1.19	5.4	0.050
6	298	180	2.23	0.67	7.3	0.068
7	285	97	1.00	0.44	6.0	0.054
8	262	91	2.87	1.02	6.8	0.056
9	250	92	2.04	1.32	7.6	0.059
10	235	92	2.76	1.09	8.4	0.061
11	227	181	1.73	0.88	11.6	0.080
12	224	93	1.77	1.11	8.2	0.056
13	223	93	2.05	0.84	8.6	0.058
14	211	92	1.60	0.80	9.1	0.058

[a] Experiment 5 was conducted using an uncoated flow tube. For all other experiments the flow tube was coated with Halocarbon wax.

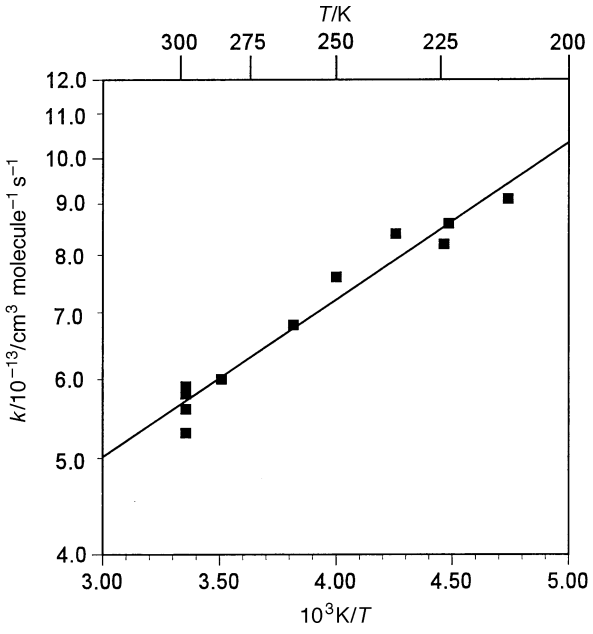

Fig. 8 Arrhenius plot for the reaction OD + ClO → DCl + O_2; the least-squares fit to the data yields the expression $k(T) = (1.7 \pm 0.3) \times 10^{-13} \exp[(363 \pm 50)/T]$ cm^3 molecule^{-1} s^{-1}

branching ratio ranges from 0.05 ± 0.02 at 298 K to 0.06 ± 0.02 at 210 K. The reported error for the branching ratio is an estimate of the systematic error and the uncertainty of the model fitting procedure based on a sensitivity analysis. The negative temperature dependence of k_{1b} indicates that reaction (1b) goes through an intermediate complex.[27,28] Mass spectral scans were recorded to investigate the possible presence of an intermediate complex, but we were unable to positively establish the existence of such a complex.

We performed some measurements of the branching ratio for the OH + ClO reaction at 298 K. These experiments were conducted with higher OH concentrations ([OH] $\approx 2 \times 10^{12}$ molecule cm^{-3}) and lower ClO concentrations ([ClO] $\approx 3 \times 10^{11}$ molecule cm^{-3}) compared to the branching ratio experiments for OD. Increasing the OH concentration made it possible to decrease the ClO concentration while still being able to produce detectable amounts of HCl from reaction (1b). The lower amounts of Cl_2 through the microwave discharge sufficiently reduced the HCl background from the ClO source, such that we were able to observe production of HCl (*ca.* 10^9 molecule cm^{-3}) over the reaction time (*ca.* 20 ms). Because the HCl background is almost an order of magnitude larger than the DCl background, the error associated with the HCl measurements is also correspondingly larger. However, the branching ratio for OH + ClO appears to be similar to our measured branching ratio for OD + ClO.

Our results for the branching ratio of reaction (1) are consistent with the results of previous studies, which are listed in Table 6. However, previous attempts to measure the branching ratio were unsuccessful in ruling out an HCl yield of zero for the minor channel, due to uncertainties in the results. Leu and Lin[9] and Burrows *et al.*[10] used chemical titration to convert the HO_2 formed by reaction (1a) back into OH, which was then detected by resonance fluorescence. The ratio of [HO_2] formed (determined by the regeneration of OH) to [OH] lost was used to calculate the branching ratio. A problem with this indirect method is that the ratio of HO_2 formed to OH lost is not exactly equal to the branching ratio due to additional loss mechanisms for HO_2, such as self-reaction or reaction with other species in the system, *i.e.* Cl, OH and ClO. Using this indirect method, Leu and Lin were able to place only an upper limit on the branching ratio. Burrows *et al.* modelled the system and found that a correction of almost 50% was necessary to convert the measured HO_2/OH ratio into a branching ratio. These authors measured the branching ratio between 243 and 298 K and found no temperature dependence. However, the large uncertainties in their results probably made it difficult for them to detect the 1% change in the branching ratio that we observed over the temperature range 210–298 K. Hills and Howard[11] were able to detect HO_2 directly using laser magnetic resonance; they measured the HO_2/OH ratio and then used modelling to extract the branching ratio, in a similar manner to Burrows *et al.* Of the four reported branching ratio studies, only Poulet *et al.*[12] were able to detect the HCl product of reaction (1b) directly using electron impact mass spectrometry by observing the HCl/OH ratio as the OH discharge was turned off and on at a fixed injector position. However, they did not have sufficient sensitivity to observe HCl production over the reaction time. As in the other studies, the errors were too large to rule out an HCl yield of zero. Because of the indirect methods used and the large reported errors, all four previous studies were unable to positively establish the existence of the minor channel.

We have positively identified reaction (1b) as a kinetically accessible product channel. In order to assess the atmospheric significance of this result, it is necessary to consider the effect of deuterium substitution on the rate of this channel. In general, substituting deuterium for hydrogen lowers the zero-point energies (ZPE) of the reactants and the intermediate complex.[27] For complex-mode reactions, if deuterium substitution lowers the ZPE of the reactants more than the ZPE of the complex, the activation energy will become less negative. Therefore, the deuterium-substituted rate will be less than the unsubstituted rate. Mozurkewich and Benson[29] used this reasoning to explain why the rate of the $DO_2 + DO_2$ reaction is slower than the rate of the $HO_2 + HO_2$ reaction.

In order to predict the kinetic isotope effect for a complex-mode reaction, the structure and properties of the intermediate complex need to be assumed or calculated, and a full Rice–Rampsberger–Kassel–Marcus (RRKM) calculation needs to be carried out. Such calculations are beyond the scope of the present work, however, our measurements of HCl production from reaction (1b) indicate that the branching ratio to produce OH instead of OD will also be of the order of

Table 6 Comparison of measured branching ratios for OH + ClO

technique[a]	T/K	P/Torr	branching ratio (k_{1b}/k_1)	ref.
DF-LF/RF	298	1.0–3.5	< 0.35	9
DF-LF/RF	243–298	1.0–5.0	0.15 ± 0.2	10
DF-LF/LMR	293	1.0	0.14 ± 0.14	11
DF-LF/EIMS	298	0.5–0.9	0.02 ± 0.12	12
DF-TF/CIMS	210–298	100	0.05 ± 0.02 at 298 K 0.06 ± 0.02 at 210 K	this work

[a] DF, discharge flow; LF, laminar flow; TF, turbulent flow; RF, resonance fluorescence detection; LMR, laser magnetic resonance detection; EIMS, electron impact mass spectrometry detection; CIMS, chemical ionization mass spectrometry detection.

5%. Several studies of termolecular reactions have shown that the isotope effect can be very small: for example, Smith and Williams[30] have studied the reactions of OH and OD with NO and NO_2 and found that the ratio $k_{OH}/k_{OD} = 1.00 \pm 0.16$ for NO and 0.99 ± 0.17 for NO_2 at 298 K and 18 Torr.

Conclusions

The results presented here provide the first positive identification of a product from reaction (1b), and therefore, we have established the kinetic significance of this minor channel. The branching ratio involving the production of DCl was determined to be 6% under stratospheric conditions, and the value for HCl is likely to be of the same order. Several modelling studies, *e.g.* by Chandra *et al.*,[5] and the more recent one by Michelsen *et al.*,[8] have proposed that a branching ratio close to 6% would resolve discrepancies between modelled and measured chlorine partitioning and ozone mixing ratios in the upper stratosphere. Our measurements for the overall rate of reaction (1) are in good agreement with the JPL recommendation at room temperature. However, we report a larger negative activation energy than the JPL recommendation by a factor of almost 2.5. Our temperature dependence is in good agreement with the work of Hills and Howard.[11] This work should help to improve modelling of O_3 levels in the upper stratosphere by placing more stringent constraints on the partitioning of stratospheric chlorine.

This research was supported by a grant from NASA Upper Atmosphere Research Program. We thank R. W. Field for the use of his high-purity deuterium gas and J.V. Brown for her assistance with the project as an Undergraduate Research Student.

References

1 G. Brasseur, A. De Rudder and C. Tricot, *J. Atmos. Chem.*, 1985, **3**, 261.
2 M. B. McElroy and R. J. Salawitch, *Science*, 1989, **243**, 763.
3 M. Natarajan and L. B. Callis, *J. Geophys. Res.*, 1991, **96**, 9361.
4 R. A. Stachnik, J. C. Hardy, J. A. Tarsala and J. W. Waters, *Geophys. Res. Lett.*, 1992, **19**, 1931.
5 S. Chandra, C. H. Jackman, A. R. Douglass, E. L. Fleming and D. B. Considine, *Geophys. Res. Lett.*, 1993, **20**, 351.
6 R. Toumi and S. Bekki, *Geophys. Res. Lett.*, 1993, **20**, 2447.
7 M. Allen and M. L. Delitsky, *J. Geophys. Res.*, 1991, **96**, 2913.
8 H. A. Michelsen, R. J. Salawitch, M. R. Gunson, C. Aellig, N. Kämpfer, M. M. Abbas, M. C. Abrams, T. L. Brown, A. Y. Chang, A. Goldman, F. W. Irion, M. J. Newchurch, C. P. Rinsland, G. P. Stiller and R. Zander, *Geophys. Res. Lett.*, 1996, **23**, 2361.
9 M. T. Leu and C. L. Lin, *Geophys. Res. Lett.*, 1979, **6**, 425.
10 J. P. Burrows, T. J. Wallington and R. P. Wayne, *J. Chem. Soc., Faraday Trans. 2*, 1984, **80**, 957.
11 A. J. Hills and C. J. Howard, *J. Chem. Phys.*, 1984, **81**, 4458.
12 G. Poulet, G. Laverdet and G. Le Bras, *J. Phys. Chem.*, 1986, **90**, 159.
13 A. R. Ravishankara, F. L. Eisele and P. H. Wine, *J. Chem. Phys.*, 1983, **78**, 1140.
14 P. O. Wennberg, R. C. Cohen, R. M. Stimpfle, J. P. Koplow, J. G. Anderson, R. J. Salawitch, D. W. Fahey, E. L. Woodbridge, E. R. Keim, R. S. Gao, C. R. Webster, R. D. May, D. W. Toohey, L. M. Avallone, M. H. Proffitt, M. Loewenstein, J. R. Podolske, K. R. Chan and S. C. Wofsy, *Science*, 1994, **266**, 398.
15 J. V. Seeley, J. T. Jayne and M. J. Molina, *Int. J. Chem. Kinet.*, 1993, **25**, 571.
16 J. V. Seeley, *Experimental Studies of Gas Phase Radical Reactions Using the Turbulent Flow Tube Technique*, PhD Thesis, Massachusetts Institute of Technology, Cambridge, MA, 1994.
17 J. V. Seeley, J. T. Jayne and M. J. Molina, *J. Phys. Chem.*, 1996, **100**, 4019.
18 J. V. Seeley, R. F. Meads, M. J. Elrod and M. J. Molina, *J. Phys. Chem.*, 1996, **100**, 4026.
19 M. J. Elrod, R. F. Meads, J. B. Lipson, J. V. Seeley and M. J. Molina, *J. Phys. Chem.*, 1996, **100**, 5808.
20 W. B. DeMore, S. P. Sander, C. J. Howard, A. R. Ravishankara, D. M. Golden, C. E. Kolb, R. F. Hampson, M. J. Kurylo and M. J. Molina, *Chemical Kinetics and Photochemical Data for Use in Stratospheric Modeling*, JPL Publication 94-26, Jet Propulsion Laboratory, Pasadena, CA, 1994.
21 W. G. Mallard, F. Westley, J. T. Herron and R. F. Hampson, *NIST Chemical Kinetics Database Version 6.0*, NIST Standard Reference Data, Gaithersberg, MD, 1994.
22 *International Critical Tables of Numerical Data: Physics, Chemistry and Technology*, ed. E. W. Washburn, New York, NY, 1928, vol. 3, p. 305.
23 J. J. Fritz and C. R. Fuget, *Chem. Eng. Data Ser.*, 1956, **1**, 10.
24 E. R. Lovejoy, T. P. Murrells, A. R. Ravishankara and C. J. Howard, *J. Phys. Chem.*, 1990, **94**, 2386.
25 L. G. Huey, D. R. Hanson and C. J. Howard, *J. Phys. Chem.*, 1995, **99**, 5001.
26 L. T. Molina and M. J. Molina, *J. Phys. Chem.*, 1987, **91**, 433.
27 J. A. Kaye, *Rev. Geophys.*, 1987, **25**, 1609.
28 J. Troe, *J. Chem. Soc., Faraday Trans.*, 1994, **90**, 2303.
29 M. Mozurkewich and S. W. Benson, *Int. J. Chem. Kinet.*, 1985, **17**, 787.
30 I. W. M. Smith and M. D. Williams, *J. Chem. Soc., Faraday Trans. 2*, 1985, **81**, 1849.

Paper 7/01946G; *Received* 19*th March*, 1997